Flow Past a Fixed and Freely Vibrating Drilling Riser System with Auxiliaries in Laminar Flow

Fatin Alias[1], Mohd Hairil Mohd[1], Mohd Azlan Musa[1], Erwan Hafizi Kasiman[2], Mohd Asamudin A Rahman[1,*]

[1] Offshore and Coastal Research Interest Group, Naval Architecture and Maritime Technology Programme, Faculty of Ocean Engineering Technology and Informatics, Universiti Malaysia Terengganu, 21030 Kuala Nerus, Terengganu, Malaysia
[2] School of Civil Engineering, Faculty of Engineering, Universiti Teknologi Malaysia, 81310 Skudai, Johor, Malaysia

ARTICLE INFO	ABSTRACT
  	Drilling risers used in oil and gas operations are subjected to external loads such as wave and current. One of the phenomena that arise from the external loads is the Vortex-Induced Vibration (VIV), which affects the performance of the riser due to excessive vibration from the vortex shedding. A significant factor influencing the VIV is the design of the drilling riser and its auxiliary lines. Until now, the optimum geometrical size and gap between the auxiliary and the main riser are still very scarcely studied. In this paper, the main objective is to study the effects of the gap ratio (G/D) on the vortex shedding phenomenon on a fixed and freely vibrating riser. The riser system was modelled with a main drilling riser and six auxiliary lines with a constant diameter ratio (d/D) of 0.45 and gap ratio (G/D) = 0 to 2.0 in the laminar flow regime with Reynold Number, Re = 200. The simulations were conducted for Single Degree of Freedom (SDOF) using Computational Fluid Dynamics (CFD) software, Altair AcuSolve. It was found that the freely vibrating riser experienced higher lift and drag forces as compared to the fixed riser due to the synchronization (lock-in) of the shedding vibration and the natural frequencies. The lock-in phenomenon is normally observed on the drilling riser at different current directions. The forces are reduced when G/D is higher. The vortex shedding was significantly reduced for auxiliaries between 0.3 to 1.4. It is confirmed that by modifying the interaction of the vortices in the wake region with auxiliary lines, the hydrodynamic forces will be decreased. Finally, this fundamental study could potentially be used in the designing stage of an optimum drilling riser system by considering significant governing factors.

1. Introduction

Vortex-Induced Vibration (VIV) of drilling risers is one of the most challenging issues in the offshore industry. VIV of riser systems is caused by cyclical shedding of vortices in the riser wake under ocean currents. It is a critical factor in designing all rigid riser systems, including drilling, manufacturing and export risers, due to high level damage and fatigue to the structure. VIV occurs

due to the interference of external fluid dynamics caused by periodic flow abnormalities. In general, the design of drilling risers has become an issue among engineers due to VIV. Thus, it is necessary to suppress VIV in the riser system [1].

Contributions towards understanding VIV have been carried out by using experiments, numerical simulation and analytical modelling [2-7]. Recently, Lou *et al.,* [8] divided the suppression devices into two categories which are, active and passive controls. For active control, power input such as rotationally oscillating cylinders was used. One of the examples of active control device is the feedback rotationally oscillating cylinders. Meanwhile, additional components were attached to the system for passive control such as control rods or auxiliaries, helical strake, fairing and splitter plate.

A previous study by Silva-Ortega and Assi [9] investigated hydrodynamic loads on a circular cylinder with two, four and eight wake-control cylinders. The experiment was conducted in the free surface channel with Reynold numbers between 5000 and 50 000. Surprisingly, it was found that the control rods with four and eight control rods, performed better than two control rods in terms of wake suppression. As highlighted by Wu *et al.,* [10], the authors examined the flow and control for a drilling riser system with auxiliary lines at various incident angles of the current flow. The study was conducted in subcritical Reynold number which is 35 000 and range of angles from 0° to 360°. They concluded that auxiliary lines could suppress the vortex shedding in all cases considered. By using the auxiliary lines, the drag coefficient on the main line was reduced and lift coefficient was also subsequently reduced. So, both the mean and root mean square (rms) values of the drag and lift coefficients were reduced effectively.

Besides, several attempts have confirmed that VIV was also affected by gap ratio and diameter ratio. For some of the latest work in this line, Papaioannou *et al.,* [11] reported the effects of the gap ratio on VIV of two tandem cylinders. Reynold number of 160 and lift-to-drag of 2.5 to 5.0 were considered in their study. When the lift-to-drag ratio increases, the lock-in regime shifts to the right-end. The dynamic behavior of the upstream and downstream cylinder did not significantly affect each other. Furthermore, the findings are consistent with the study by Lu *et al.,* [12] which found that the cylinder group acted as a single body under a very low gap ratio. However, the effective dimension of the system was enhanced due to the presence of small control rods that led to a wider wake area with small pressure at the centre of the main vortex. Hence, higher mean drag force and lift fluctuation on the main cylinder were observed compared to an independent circular cylinder. Moreover, Zhao *et al.,* [13] had performed numerical simulation of flow past a main circular cylinder with one small control cylinder. The effects of the position angle of the small cylinder and the gap ratio between the two cylinders on force coefficients, pressure distributions and flow patterns were studied. They found that the drag force and lift force can be significantly reduced if the rod is placed at the proper position. Therefore, vortex shedding can be classified into three types which are single-wake shedding mode, interaction mode and two-wake mode. Each type is categorized by a very small gap ratio, medium gap ratio and a very large gap ratio.

Accordingly, the aim of the present work is to investigate the flow past a fixed and freely vibrating cylinder in a drilling riser with auxiliary system on the VIV phenomenon. The analysis of the hydrodynamic forces and response amplitude of a fixed and freely vibrating circular cylinder were crucial and discussed in this paper. The gap ratios that are considered in this study varies from 0 to 2.0 with constant diameter of 0.45. The Reynold Number (Re) is constant at 200 for the simulation.

2. Methodology

2.1 Computational Meshing and Boundary Condition

Figure 1 illustrates a rectangle computational domain of a circular cylinder with six identical circular cylinders located around a main cylinder. The gap ratio and diameter ratio are defined in Eq. (1) and Eq. (2), where G is the gap or distance between the surface of the main cylinder and the surface of each control rod. D is the diameter of the main cylinder while d is the diameter of auxiliaries. The range for gap ratio considered in this study is between 0 and 2.0 with a constant diameter ratio of 0.45. The simulation was focused on a Single Degree of Freedom (SDOF) only. The elastic system consists of a damping constant, c and spring damper, k. By using a spring damper system, the cylinder was allowed to vibrate in the cross-flow direction. In this paper, the cylinder is considered as a rigid riser and allowed to be displaced in cross-flow direction. The simulations were conducted for the Reynold Number, Re=200 which correspond to a range of reduced velocity V_r = 2-18 (Eq. (3)). Natural frequency was calculated using Eq. (4) while Eq. (5) and Eq. (6) calculate mass ratio and damping, respectively. Time step used is 0.05 which converged smoothly for the case studied. The time integration errors are found insignificant. Physical parameter values utilized in the present study are tabulated in Table 1.
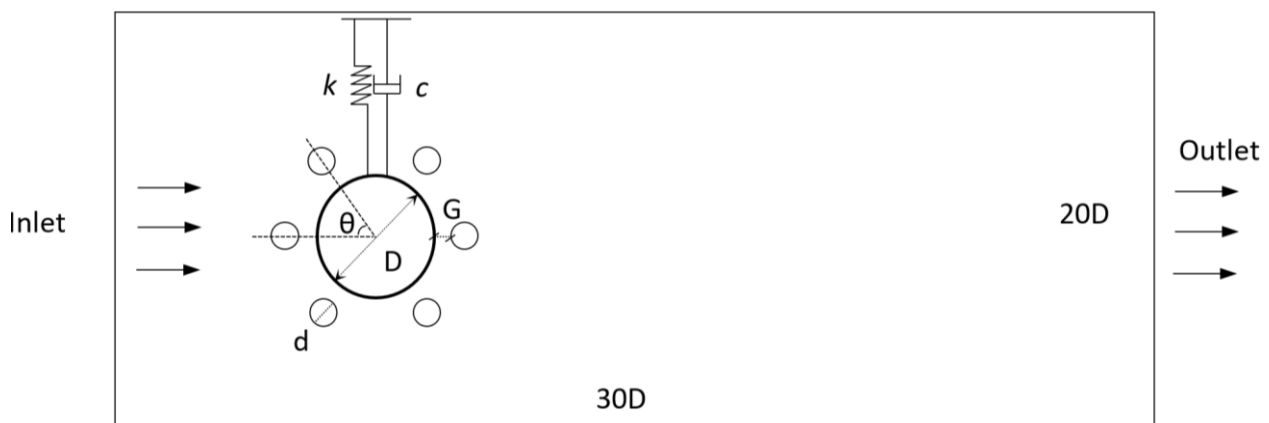

Fig. 1. Schematic drawing of the drilling riser with six auxiliaries (not to scale)

Table 1
Physical Parameter Values

Parameter	Symbol	Value	Units
Gap ratio	$\dfrac{G}{D}$	0 – 2.0	-
Diameter ratio	$\dfrac{d}{D}$	0.45	-
Angle	θ	0	° (degree)
Reynold Number		200	
Mass ratio	$m*$	2.0	
Damping	ζ	0.007	
Reduced velocity	V_r	2-18	

$$Gap\ ratio, = \frac{G}{D} \tag{1}$$

$$Diameter\ ratio, = \frac{d}{D} \tag{2}$$

$$U_r = \frac{U}{f_d D} \tag{3}$$

$$f_n = \frac{1}{2\pi}\sqrt{\frac{k}{m}} \tag{4}$$

$$m^* = \frac{4m}{\rho \pi D^2} \tag{5}$$

$$\zeta = \frac{c}{2\sqrt{km}} \tag{6}$$

The boundary conditions of the domain were defined as shown in Table 2. At the inlet boundary, the mean velocity of the uniform flow was defined which corresponded to Reynold Number of 200. Slip wall was assigned to the wall boundaries to simulate the boundaries of the pressure outlet where there was no shear stress between the fluid and walls. Then, the outlet was defined where no viscous stress was considered.

Table 2
The boundary conditions of the CFD model

Type of boundary	Surface Name
Wall	Main cylinder, auxiliaries
Slip	Sides
Symmetry	Top, Bottom
Inflow	Inlet
Outflow	Outlet

2.2 Mesh Independence Study of Vibrated Single Cylinder

A convergence test was performed to obtain a stable solution for the numerical models. Figure 2 shows the mesh configurations for the simulation domain. Meanwhile, Figure 3 shows the mesh study conducted for the various number of element. From the graph, it can be seen that the simulations started to converge around A_y/D = 0.06468 at around 132 000 number of element. The results for the amplitude response shows a good agreement with data published by Carmo *et al.,* [14].
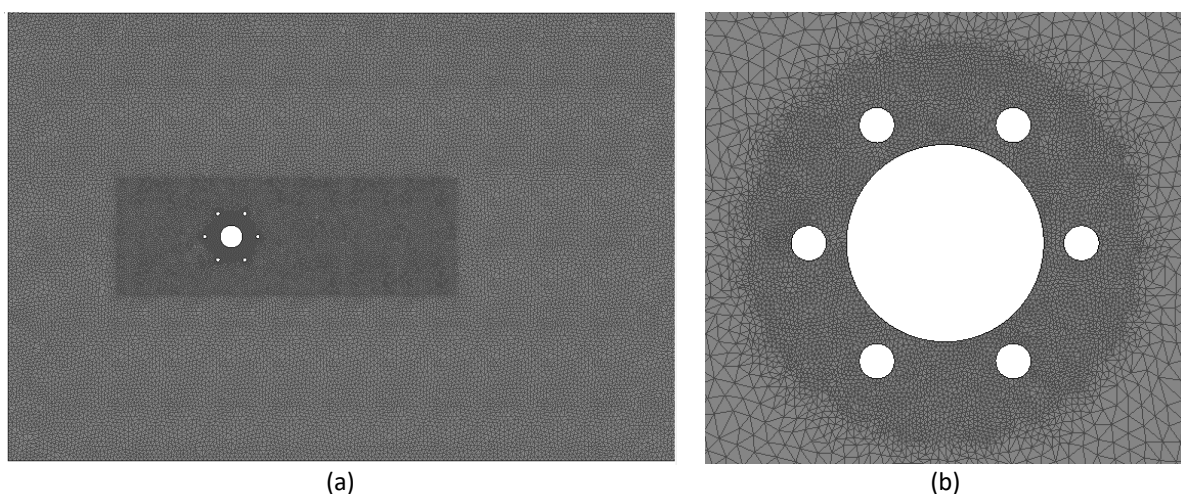

(a)   (b)

Fig. 2. (a) Computation meshes of a main cylinder with six auxiliaries; (b) Illustration of the mesh for case *d/D*= 0.45 and *G/D* = 0.04
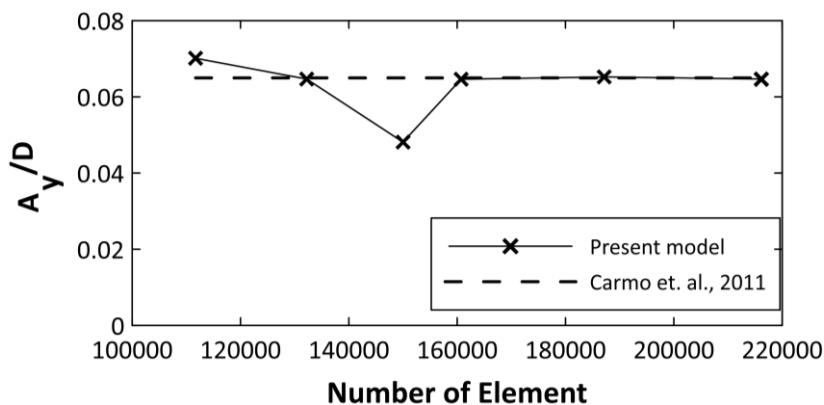
Fig. 3. Mesh Convergence Study of a single vibrating cylinder with different mesh elements

2.3 Model Validation

Validation is performed to verify the feasibility and efficiency of the computational method of the current CFD model. Simulation of the single cylinder at Re=150 was conducted and the results were compared to the published data. Based on Figure 4, a comparison was made with Carmo *et al.,* [14]. By using the results obtained, the findings are found to be in good agreement. The maximum relative error is found to be less than 5%. The numerical results show that the amplitude on a single cylinder was reduced significantly as the reduced velocity increases.
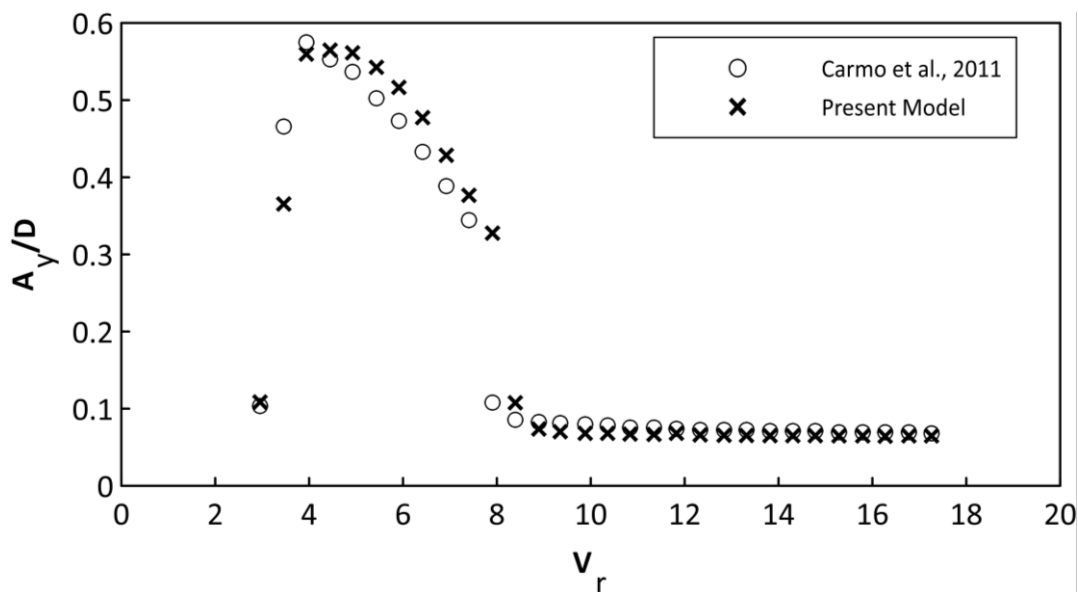

Fig. 4. Comparison and validation between present model and Carmo *et al.,* [14] for mean Drag coefficient and rms Lift Coefficient of a main cylinder and six auxiliaries at Re= 200

3. Results and Discussion

Table 3 illustrates the gap ratio that was divided into five regimes to ease the discussion of the result. The selection of the regime was based on the characteristics of the hydrodynamic forces at different gap ratios. The discussion is based on Figure 5 to Figure 8. Figure 5 shows the maximum amplitude corresponding to transverse amplitude. The maximum amplitude is defined as the mean of the top 10% of half peak-to-peak values. Figure 6 shows graphs of mean drag Coefficient, $C_{D\,(mean)}$

for different gap ratios while Figure 7 shows rms lift Coefficient, $C_{L\ (rms)}$ for different gap ratios for fixed and vibrating cylinder. For Figure 8, the vorticity contour in velocity magnitude of a main cylinder with six auxiliaries at different incidence angles is shown.

Table 3
Range of Regime

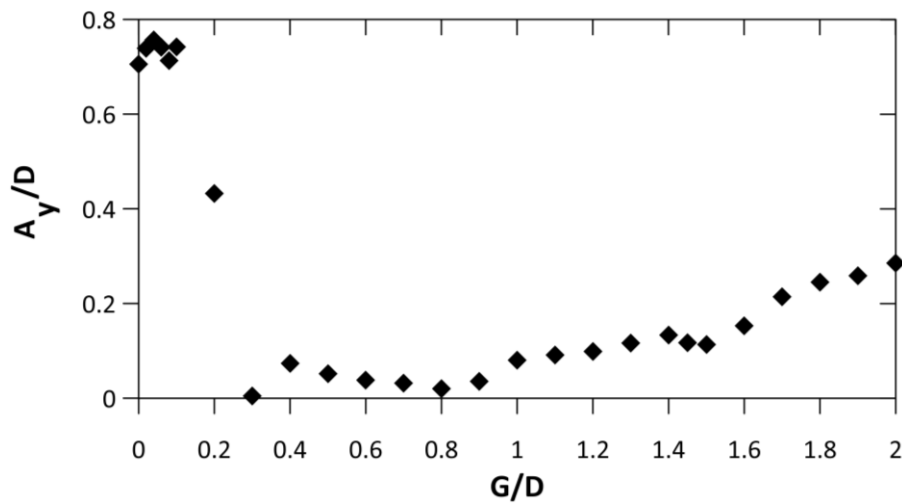| Regime	Range
1	$0 \leq G/D \geq 0.1$
2	$0.1 < G/D \geq 0.3$
3	$0.3 < G/D \geq 1.4$
4	$1.4 < G/D < 1.5$
5	$G/D \geq 1.5$

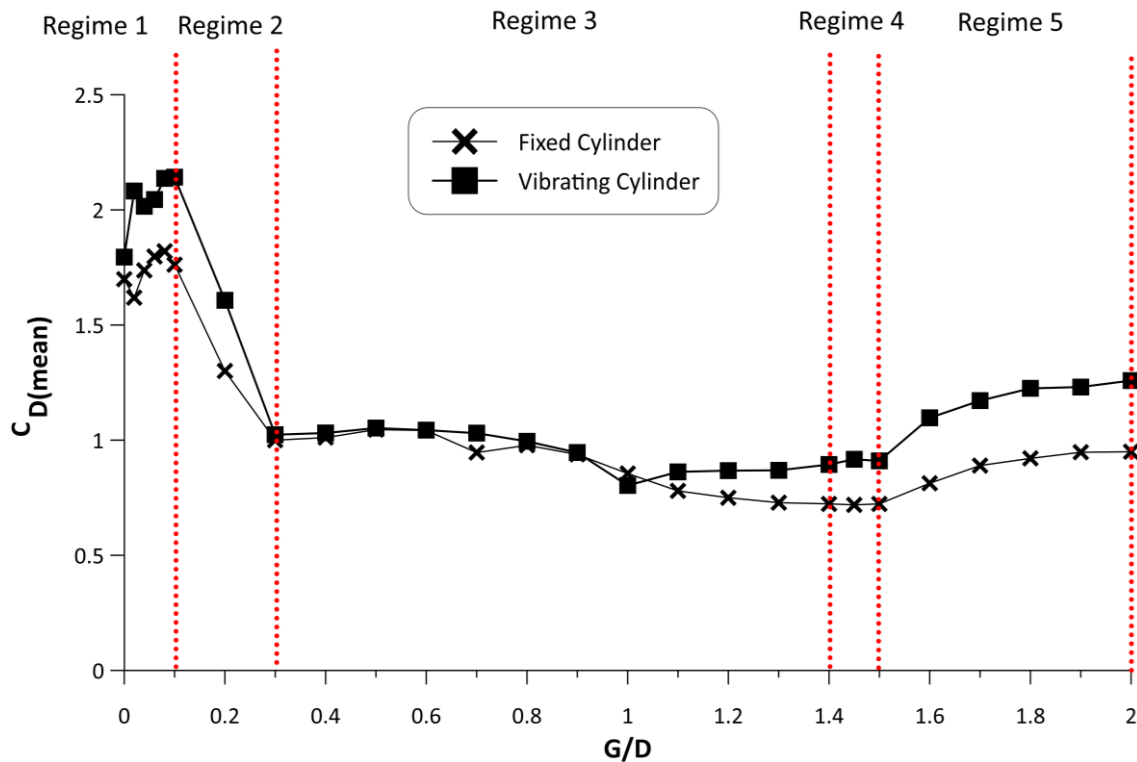**Fig. 5.** Maximum amplitude (cross-flow direction) for different gap ratios

Fig. 6. Mean Drag Coefficient for fixed and vibrating cylinder with different gap ratios
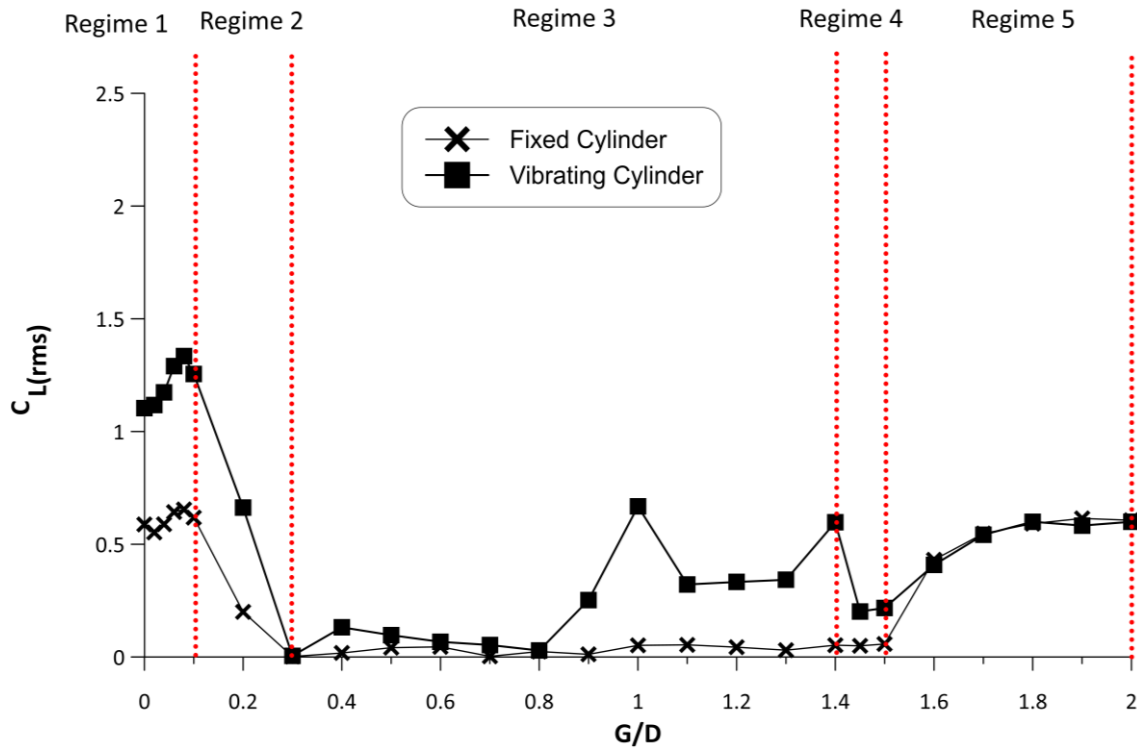
Fig. 7. rms Lift Coefficient for fixed and vibrating cylinder with different gap ratios

The drag coefficient (C_D) and Lift coefficient (C_L) were calculated using Eq. (9) and Eq. (10) [10].

$$C_D = \frac{2F_x}{\rho U^2 D} \tag{9}$$

$$C_L = \frac{2F_y}{\rho U^2 D} \tag{10}$$

where F_x and F_y are fluid forces, in the in-line direction and the cross-flow direction. ρ is the density of the fluid, U is the time-average velocity vector of the fluid and D is the diameter of the main cylinder. Meanwhile, Eq. (11) and Eq. (12) show the mean drag coefficient ($C_{D\ (mean)}$), root mean square (rms) and lift coefficient ($C_{L\ (rms)}$).

$$C_{D\ (mean)} = \frac{1}{N}\sum_{n=1}^{N} C_D \tag{11}$$

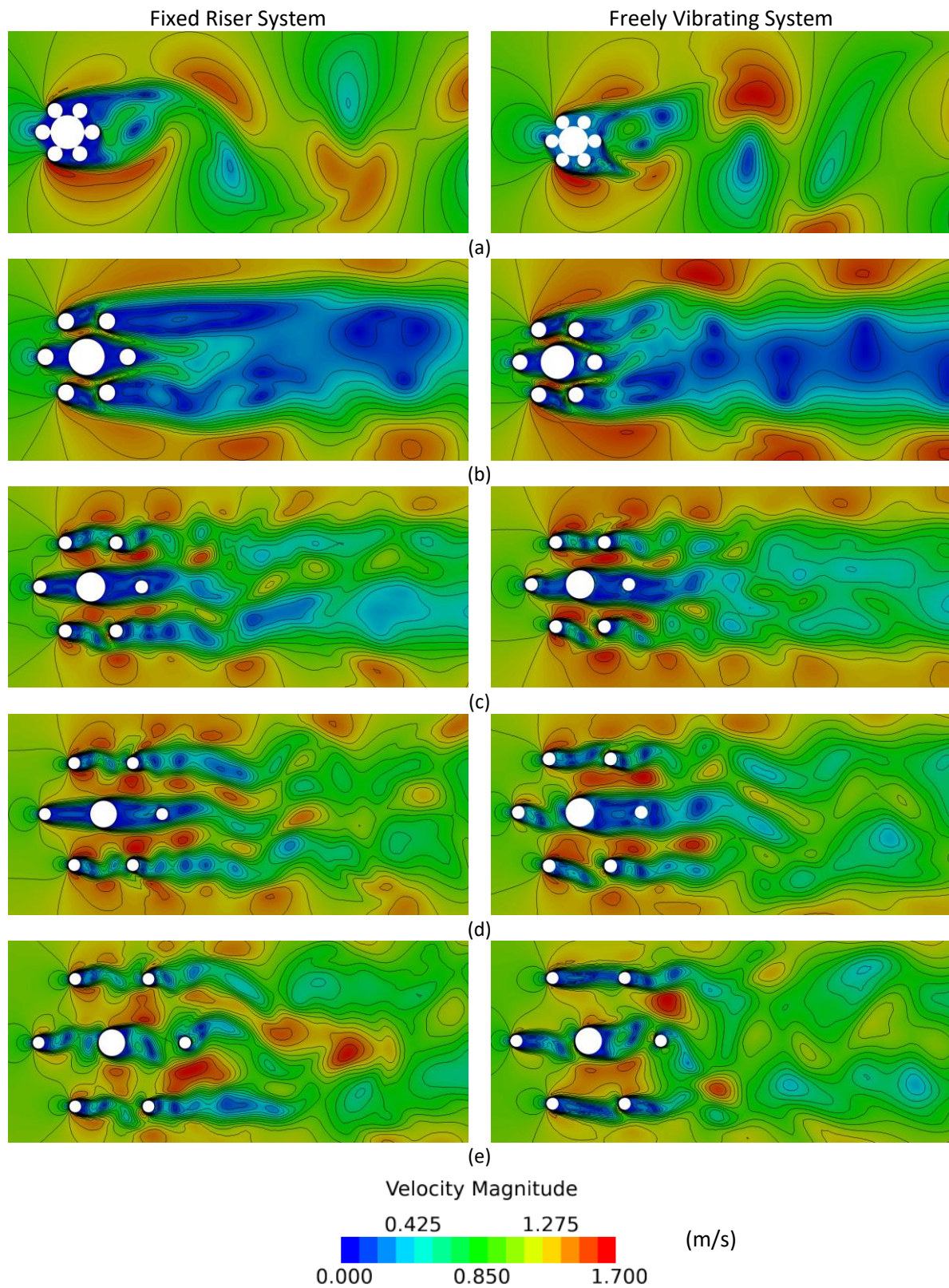$$C_{L\ (rms)} = \sqrt{\frac{1}{N}\sum_{n=1}^{N}(C_L - \overline{C_L})^2} \tag{12}$$

Fig. 8. Vorticity Contour for five different Regimes; (a) Regime 1, (b) Regime 2, (c) Regime 3, (d) Regime 4

For Regime 1, $C_{D\ (mean)}$ increases at *G/D*=0-0.1. The maximum value of $C_{D\ (mean)}$ for vibrating cylinder is 1.33398 and 1.82000 for fixed cylinder. The increase of the drag is due to the increasing stagnation pressure and the high pressure on the front of the main cylinder. The graph shows that there has been sharp rise of $C_{L\ (rms)}$ for all *G/D* in Regime 1. $C_{L\ (rms)}$ is at peak when *G/D* is 0.08 for both fixed and vibrating cylinder. This phenomenon is due to the disturbance from the six auxiliary lines to the formation of the shear layer on the upstream face of the main cylinder and the interaction of the shear layer in the wake region of the main cylinder. Based on Figure 8(a), the *Kármán Vortex Street* is found as the vortex sheds. The increase of vortex size and vortex shedding are based on gap ratios. The vortices at the upstream is stronger than downstream which is in good agreement with Zhu and Gao [15]. The A_y/D of Regime 1, shows the highest amplitude compared to others which has the average of 0.73283.

In Regime 2, $C_{D\ (mean)}$ decreases when *G/D* increases. The total reduction is 41%. This is due to the separation point along the surfaces of the main cylinder. Besides, Silva-Ortega and Assi [9] found that the gap ratio is significant to the results of the $C_{D\ (mean)}$. The higher the gap ratio, the lower the drag force. $C_{L\ (rms)}$ then, reduces then converge close to zero at *G/D* 0.3. This causes A_y/D to also be reduced in Regime 2. Three streets can be identified in Figure 8(b) due to auxiliaries immersed in the shear layer of the main cylinder. All the vortices are cancelled out in the wake and $C_{L\ (rms)}$ values and amplitude of the main cylinder are reduced.

At Regime 3, $C_{D\ (mean)}$ continues to decrease when the gap ratio increases. The value of $C_{D\ (mean)}$ of the fixed and vibrating cylinder are the same. This reduction occurs due to the wake suppression that is more efficient at a low gap ratio. The findings are supported by Zhu *et al.,* [16] where it shows that the increase of gap ratio leads to the wake to become wider as a result of less injected momentum into the boundary layer thus, the wake-flow control is not achieved in that case. $C_{L\ (rms)}$ is also, significantly reduced. The minimum $C_{L\ (rms)}$ is 0.00304 for fixed cylinder and 0.0201 for vibrating cylinder. The existence of the six auxiliaries in the wake of a main cylinder delays the interaction of the shear layer behind the main cylinder. Based on Figure 8(c) and Figure 8(d), three vortex streets are recognized because of the increase in gap ratio. The three classes of the vortices seem to be dispersed independently. Additionally, it can be observed that there is a strong interaction among the streets. The three vortex shedding processes are in-phase among each other. Lu *et al.,* [12] also showed similar findings where three vortex streets appeared because the gap ratio increased.

For Regime 4, $C_{D\ (mean)}$ increases at *G/D* = 1.0, for both fixed and vibrating cylinder. The unstable of drag and lift in the data is probably due to the beat of motion in the time series acquired in the simulation. However, the value of $C_{D\ (mean)}$ and $C_{L\ (rms)}$ are in range. Lastly, for Regime 5, the presence of the auxiliaries prevents the interaction of the vortices across the centre line of the wake (in Figure 8(e)). This condition will affect the $C_{D\ (mean)}$ of the main cylinder. The vortex shedding is taking place in the close wake of the main cylinder. It can also be observed that the hydrodynamics forces of a main cylinder are dependent on the flow instability and wake modes. Furthermore, Song *et al.,* [17] reveals that the best suppression occurred when they use three auxiliary lines. Therefore, the three auxiliaries were better than one auxiliary to suppress the VIV.

4. Conclusions

This study was undertaken to determine the effects of the gap and the diameter ratio of a drilling riser with auxiliaries on the vortex shedding phenomenon. This study shows that five flow regimes can be identified by varying the gap at Re=200. It was found that the freely vibrating riser experienced

higher lift and drag forces compared to the fixed riser due to high frequencies of hydrodynamics forces fluctuations on the main cylinder. In Regime 1, both means drag and rms lift coefficients increased. Then, the hydrodynamic coefficients decreased when the gap ratio increased in Regime 2 and 3. As the gap ratio increased in Regime 4, the mean drag and rms lift coefficients show a significantly high value. Meanwhile, in Regime 5, vortex shedding phenomenon independently occurred without the effect from auxiliary lines. The results of this investigation show that the drag and lift components were reduced in the range of gap ratio $0.3 < G/D < 1.4$. Meanwhile, a larger diameter ratio of $0.35 < d/D < 0.5$ shows a significant reduction of the mean drag in the same gap ratio range. Considered as a whole, these observations suggest that the optimum gap ratios for the drilling riser with auxiliary lines can be designed within the suggested ratios, in order to suppress the vortex shedding phenomenon on the main drilling riser. For the future, optimization study on the auxiliaries of a drilling riser should be carried out in order to design an optimum riser system with low vulnerability to the VIV phenomenon.

Acknowledgement

References

[1] Wu, Wenbo, and Jiasong Wang. "Numerical simulation of VIV for a circular cylinder with a downstream control rod at low Reynolds number." *European Journal of Mechanics-B/Fluids* 68 (2018): 153-166. https://doi.org/10.1016/j.euromechflu.2017.12.005

[2] A Rahman, Mohd Asamudin, Wan Norazam Wan Hussin, Mohd Hairil Mohd, Fatimah Noor Harun, Lee Kee Quen, and Jeom Kee Paik. "Modified wake oscillator model for vortex-induced motion prediction of low aspect ratio structures." *Ships and Offshore Structures* 14, no. sup1 (2019): 335-343. https://doi.org/10.1080/17445302.2019.1593308

[3] Kang, Zhuang, Cheng Zhang, Rui Chang, and Gang Ma. "A numerical investigation of the effects of Reynolds number on vortex-induced vibration of the cylinders with different mass ratios and frequency ratios." *International Journal of Naval Architecture and Ocean Engineering* 11, no. 2 (2019): 835-850. https://doi.org/10.1016/j.ijnaoe.2019.02.012

[4] Gsell, Simon, Rémi Bourguet, and Marianna Braza. "Two-degree-of-freedom vortex-induced vibrations of a circular cylinder at Re= 3900." *Journal of Fluids and Structures* 67 (2016): 156-172. https://doi.org/10.1016/j.jfluidstructs.2016.09.004

[5] Chen, Mengyue, Xiuquan Liu, Fulai Liu, and Min Lou. "Optimal design of two-dimensional riser fairings for vortex-induced vibration suppression based on genetic algorithm." *arXiv preprint arXiv:1801.03792* (2018).

[6] Zhou, Tongming, S. F. Mohd Razali, Z. Hao, and Liang Cheng. "On the study of vortex-induced vibration of a cylinder with helical strakes." *Journal of Fluids and Structures* 27, no. 7 (2011): 903-917. https://doi.org/10.1016/j.jfluidstructs.2011.04.014

[7] Rahman, Mohd Asamudin A., Muhammad Nadzrin Nazri, Ahmad Fitriadhy, Mohammad Fadhli Ahmad, Erwan Hafizi Kasiman, Mohd Azlan Musa, Fatin Alias, and Mohd Hairil Mohd. "A Fundamental CFD Investigation of Offshore Structures for Artificial Coral Reef Development." *CFD Letters* 12, no. 7 (2020): 110-125. https://doi.org/10.37934/cfdl.12.7.110125

[8] Lou, Min, Wu-gang Wu, and Peng Chen. "Experimental study on vortex induced vibration of risers with fairing considering wake interference." *International Journal of Naval Architecture and Ocean Engineering* 9, no. 2 (2017): 127-134. https://doi.org/10.1016/j.ijnaoe.2016.08.006

[9] Silva-Ortega, M., and G. R. S. Assi. "Hydrodynamic loads on a circular cylinder surrounded by two, four and eight wake-control cylinders." *Ocean Engineering* 153 (2018): 345-352. https://doi.org/10.1016/j.oceaneng.2018.01.116

[10] Wu, Wenbo, Jiasong Wang, Shiquan Jiang, Liangbin Xu, and Leixiang Sheng. "Flow and flow control modeling for a drilling riser system with auxiliary lines." *Ocean Engineering* 123 (2016): 204-222. https://doi.org/10.1016/j.oceaneng.2016.06.043

[11] Papaioannou, G. V., D. K. P. Yue, M. S. Triantafyllou, and G. E. Karniadakis. "On the effect of spacing on the vortex-induced vibrations of two tandem cylinders." *Journal of Fluids and Structures* 24, no. 6 (2008): 833-854. https://doi.org/10.1016/j.jfluidstructs.2007.11.006

[12] Lu, Lin, Ming-ming Liu, Bin Teng, Zhen-dong Cui, Guo-qiang Tang, Ming Zhao, and Liang Cheng. "Numerical investigation of fluid flow past circular cylinder with multiple control rods at low Reynolds number." *Journal of Fluids and Structures* 48 (2014): 235-259. https://doi.org/10.1016/j.jfluidstructs.2014.03.006

[13] Zhao, Ming, Liang Cheng, Bin Teng, and Dongfang Liang. "Numerical simulation of viscous flow past two circular cylinders of different diameters." *Applied Ocean Research* 27, no. 1 (2005): 39-55. https://doi.org/10.1016/j.apor.2004.10.002

[14] Carmo, B. S., S. J. Sherwin, P. W. Bearman, and R. H. J. Willden. "Flow-induced vibration of a circular cylinder subjected to wake interference at low Reynolds number." *Journal of Fluids and Structures* 27, no. 4 (2011): 503-522. https://doi.org/10.1016/j.jfluidstructs.2011.04.003

[15] Zhu, Hongjun, and Yue Gao. "Effect of gap on the vortex-induced vibration suppression of a circular cylinder using two rotating rods." *Ships and Offshore Structures* 13, no. 2 (2018): 119-131. https://doi.org/10.1080/17445302.2017.1328756

[16] Zhu, Hongjun, Jie Yao, Yue Ma, Hongnan Zhao, and Youbo Tang. "Simultaneous CFD evaluation of VIV suppression using smaller control cylinders." *Journal of Fluids and Structures* 57 (2015): 66-80. https://doi.org/10.1016/j.jfluidstructs.2015.05.011

[17] Song, Zhenhua, Menglan Duan, and Jijun Gu. "Numerical investigation on the suppression of VIV for a circular cylinder by three small control rods." *Applied Ocean Research* 64 (2017): 169-183. https://doi.org/10.1016/j.apor.2017.03.001